Thermal Performance Analysis of an Artificially Roughened Solar airborne heater with Ribs: A CFD Analysis

T.S.V. Vijay Murali, I.V. Kumar, M. Mohan Jagadeesh Kumar

Abstract— Heat transfer coefficients in solar airborne heaters have to be passively upgraded by building turbulence near its absorbent plate. Turbulence near the plate can be augmented by attaching synthetic ribs of different geometries to its surface. In this paper numerical investigations are carried out and results are presented by simulating flow through solar airborne heater as continuous flow into a rectangular shaped duct with artificially ribbed bottom most surface. Ribs of dissimilar cross-sections including triangular, semi-circular, rectangular and arc in shape are considered for the numerical analysis. Constant heat flux boundary condition is being used at the bottom most surface of the rectangular shaped duct. Heat transfer rates for flow through rectangular shaped duct with plane bottom most surface are compared with corresponding values with ribbed bottom most surface. Reynolds number (2300-20000), relative roughness pitch (6.67, 10, 13.33) and relative roughness altitude (0.055, 0.073, 0.11) are considered as parametric variables. Heat transfer rates are found to be increased for ribbed rectangular bottom most surface compared to plane rectangular surface. Arc shaped ribs are giving higher augmentation in heat transfer through duct compared to rectangular, triangular and semi-circular ribs. Arc shaped ribs with a relative roughness altitude of 0.055 and relative roughness pitch of 10 increasing Nusselt number by 1.66 times comparing with plane surface. Arc shaped ribs with same relative roughness pitch increases Nusselt number by 1.78 and 1.48 times with relative roughness altitude equal to 0.073 and 0.11 respectively.

Keywords: Absorber plate, Heat transfer coefficient, Reynolds number, Solar airborne heater.

1. INTRODUCTION

In 21st century with increase in global warming effect it is necessary to develop pollution free energy generation methods. Energy available in solar radiation substitute conventional sources and can be utilized to develop clean energy conversion systems. Major advantage is availability of solar radiation in abundant at free of cost across the globe. Solar electrical energy conversion systems are two categories: direct and indirect. In direct energy conversion solar systems, photovoltaic cells are used to transform solar power radiation into electricity. In indirect energy conversion solar systems solar collectors, solar ponds etc. are initially used to transform solar power radiation into thermal power and then conventional Rankine cycle engines are used to convert thermal energy to electricity. Applications of solar energy also include thermal heat generation, space heating, refrigeration and air-conditioning, drying/curing of agricultural products, air heating etc. The two basic limitations of the solar energy are: (a) availability of solar energy is discontinuous and (b) area required to collect the solar energy is very large.

Many researchers developed techniques to run the solar based applications round the clock by absorbing/storing the solar energy during its available time and use the same effectively in its unavailable time. Huge technical advancement in the material science and technology made the applications of solar energy at lower price. Solar airborne heater as in Fig. 1 is a rectangular shape duct with transparent glass cover at its top. An absorber plate coated with black paint is placed at its bottom side. Bottom and sides are completely insulated. Solar radiation passes through glass cover convert into heat by absorption at the absorber. Atmospheric air is allowed to pass through air heater to receive heat by convection from the absorber plate.

Industrial presentations like space heating, timber seasoning; curing of industrial oriented products, agricultural product drying etc. requires hot air to remove moisture. Solar airborne heaters prepared at low price, simple in its operation can supply hot air for such industrial applications.

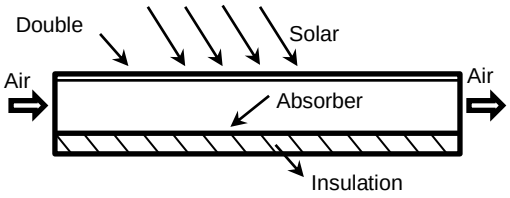

Fig. 1 Solar airborne heater

Thermal power performance of a solar airborne heater is low due to low heat transferal coefficients with air as a working medium in solar airborne heaters. Theoretical and experimental analyses are carried out on solar airborne heaters across the globe to enhance heat transfer coefficients with different passive and active techniques.

Revised Version Manuscript Received on April 05, 2019.

T.S.V. Vijay Murali, M.Tech Student, Gayatri Vidya Parishad College of Engineering (A), Andhra Pradesh, India (E-mail: vijay.murali1994@gmail.com)

I.V. Kumar, M.Tech Student, Gayatri Vidya Parishad College of Engineering (A), Andhra Pradesh, India(E-Mail: ivkumar066@gmail.com)

M. Mohan Jagadeesh Kumar, Associate Professor, Gayatri Vidya Parishad College of Engineering (A), Andhra Pradesh, India (E-Mail: mohan_mandapati@gvpce.ac.in0

2. REVIEW OF LITERATURE

Research is being carried out from past few decades to improve heat transfer coefficients and hence to utilize maximum amount of energy available from the solar radiation. The most recognized passive techniques to augment heat transfer coefficients in Solar airborne heaters (SAHs) is the implementation of protrusions/ribs on its absorber plate. Ribs used will obstruct the air flow and causes turbulence near the absorber place and hence heat transfer coefficients will be increased. Some key research and developments under this category are discussed here.

Experiments are conducted on SAHs to know the improvement in heat transfer rate by providing ribs on either side of its absorber plate. Varun *et al.* [1] conducted experiments and found that SAH is giving better performance with transverse ribs over the plate at relative roughness pitch equal to eight. Prasad and Saini [2] conducted experiments by providing small diameter protrusion wires on the absorber plate to improve heat transfer rates in SAH. Gupta *et al.* [3] carried experimental investigations over absorber plate with transverse wires on its bottom side. Experimental investigations are conducted on SAH with W-shaped ribs by Atul Lanjewar *et al*. [4], rectangular ribs by Abdul-Malik Ebrahim Momin *et al*. [5] and inclined square split ribs by Gandhi et al. [6]. It is found that heat transfer coefficients and friction factor increases with increase in relative roughness altitude of the ribs [4, 5]. Efficiency of SAH is found to be the maximum for the relative gap position of 0.25 and the relative gap width of 1.0. Gill *et al.* [7] conducted experiments on SAH with broken arc ribs in staggered grid format and found that performance of SAH is higher for relative staggered rib size of four. An artificially roughened SAH having aspect ratio of 12 is experimentally investigated by Khushmeet *et al*. [8] and found that Nusselt number is maximum for relative roughness altitude equal to 0.043, arc angle of 60° and relative roughness pitch equal to 8. Efficiency of SAH with non-uniform cross-sectioned square profiled transverse ribs is found to be maximum for a relative roughness altitude of 10 and Reynold number equal to 12000 from an experimental investigation by Inderjeet and Sukhmeet [9].

Numerical investigations using different turbulent flow models in ANSYS FLUENT are being carried out by considering the flow through the SAH is turbulent. Review on turbulent flow analysis for flow through SAH is presented in Anil and Bhagoria [10]. Numerical investigations are carried out by Kumar and Saini [11] by providing thin circular wire shaped ribs over the absorber plate of SAH. Tabish Alam and Man-Hoe Kim [12]-[13] performed numerical investigations by providing conical protrusions and found better performance of SAH at relative roughness altitude of 0.044 and relative roughness pitch of 10. Similar investigations are carried out by same authors considering semi elliptical obstacles over the absorber plate and concluded that ribs in staggered arrangement are giving better performance compared to their regular arrangement. Parametric analysis of SAH provided with V-shaped ribs on the absorber plate is done by Dongxu Jin *et al.* [14] using ANSYS FLUENT. Nusselt number and friction factor are found to be increased by 1.78 and 2.49 times respectively for a SAH provided with saw tooth ribs compared to SAH with plane absorber plate, Sukhmeet *et al*. [15]. The effect of relative gap width and angle of attack on heat transfer through SAH with square ribs is numerical tested by Aharwal *et al*. [16]. SAH with equilateral triangular ribs on its absorber plate is numerically tested using RNG k-$\mathcal{E}$ turbulent model by Yadav and Bhagoria [17]. Similar analysis for flow through SAH with broken arc ribs is conducted by Hans *et al*. [18] and performance of SAH is found to be higher at relative roughness altitude of 0.043. Higher heat transfer augmentation is found in numerical investigations by Alok *et al*. [19] for flow through rectangular shaped ducts with chamfered ribs on its absorber plate compared to rectangular ribs. Flow through a SAH with transverse ribs is numerically investigated using ANSYS FLUENT with k-ε RNG, k-ε standard, k-ε SST, k-ε RZ models by Boulemates *et al.* [20]. Higher heat transfer rates with rib turbulators in staggered arrangement are observed for flow through SAH in a numerical investigation by Sompol *et al*. [21]. The optimum values of relative height and pitch are obtained as 0.4 and 0.5 respectively for higher heat transfer rates. Better heat transfer rates for flow through a SAH with reverse L-shaped ribs on its absorber plate are obtained at at p/e of 7.14 and e/D of 0.042 at Re of 15000 from numerical investigations by Vipin *et al*. [22]. Lakshmipathi and Mohan [23] proposed the use of SAH in a Jaggery making unit to remove moisture content from bagasse and improve its thermal efficiency.

It was found from the literature that the analysis of SAH with arc ribs is not presented. In the present article SAH with arc shaped ribs on its absorber plate are proposed to improve its conversion efficiency and flow through SAH is numerically compared with conventional ribs.

3. NUMERICAL SIMULATION

In the present analysis Solar airborne heater (SAH) with dimensions 0.3 m×0.5 m×0.03 m is considered. In the present study only test section is considered for the analysis, although conventional SAH is having diverging and converging sections at its ends. Fig. 2 shows the line diagram of the four different profiles shapes of the ribs considered for the present study.

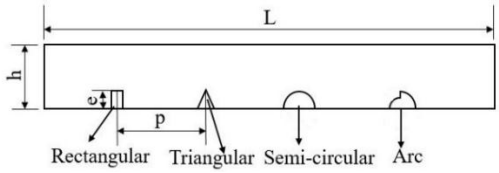

Fig. 2 Rib profiles considered for the analysis

Material for the SAH duct and working fluid passing through the SAH are aluminum and air respectively. Properties of material, working fluid and parametric variables considered for the analysis are given in Table I and Table II respectively.

Height of the rib when assessed with hydraulic diameter of the rectangular shaped duct is considered as Relative roughness altitude (e/D_h). Pitch in comparison to height of the ribs is considered as Relative

Table I Properties of Aluminum and Air

Parameter	Aluminum	Air
Density, ρ	2719	1.17
Specific Heat, C_p	871	1007
Thermal conductivity, k	202.39	0.0259
Prandtl number, Pr	--	0.7069
Viscosity, μ	--	0.00001857

Table II Parametric variables considered for the present analysis

Reynolds number, Re	2300 to 20000
Relative roughness altitude, e/D_h	0.0549, 0.0729 and 0.109
Relative roughness pitch, p/e	6.659, 10 and 13.329
Heat flux, q″, W/m^2	1000

roughness pitch (p/e). With known values of cross sectional area ($A_{c/s}$) and perimeter (P) of the duct hydraulic diameter is calculated using Eq. (1).

$$D_h = \frac{4A_{C/S}}{P} \tag{1}$$

A. Governing equations

Applying the conservation principles flow through SAH is analyzed with the following governing equations,

Conservation of mass:

$$\frac{\partial \rho}{\partial t} + \frac{\partial}{\partial x}(\rho u) + \frac{\partial}{\partial y}(\rho v) + \frac{\partial}{\partial z}(\rho w) = 0 \tag{2}$$

Conservation of momentum:

$$\rho\frac{\partial u}{\partial t} + \rho u\frac{\partial u}{\partial x} + \rho v\frac{\partial u}{\partial y} + \rho w\frac{\partial u}{\partial z} = -\frac{\partial p}{\partial x} + \mu\nabla^2 u \tag{3}$$

$$\rho\frac{\partial v}{\partial t} + \rho u\frac{\partial v}{\partial x} + \rho v\frac{\partial v}{\partial y} + \rho w\frac{\partial v}{\partial z} = -\frac{\partial p}{\partial y} + \mu\nabla^2 v \tag{4}$$

$$\rho\frac{\partial w}{\partial t} + \rho u\frac{\partial w}{\partial x} + \rho v\frac{\partial w}{\partial y} + \rho w\frac{\partial w}{\partial z} = -\frac{\partial p}{\partial z} + \mu\nabla^2 w \tag{5}$$

$$\frac{\partial}{\partial t}(\rho k) + \frac{\partial}{\partial x_j}(\rho k u_j) = \frac{\partial}{\partial x_j}\left[(a_k \mu_{eff})\frac{\partial k}{\partial x_j}\right] + G_k + G_b - \rho\varepsilon - Y_M + S_k \tag{6}$$

$$\frac{\partial}{\partial t}(\rho\varepsilon) + \frac{\partial}{\partial x_j}(\rho\varepsilon u_j) = \frac{\partial}{\partial x_j}\left[(a_\varepsilon \mu_{eff})\frac{\partial \varepsilon}{\partial x_j}\right] - C_{2\varepsilon}\rho\frac{\varepsilon^2}{k} + C_{1\varepsilon}\frac{\varepsilon}{k}(G_k + C_{3\varepsilon}G_b) - R_\varepsilon + S_\varepsilon \tag{7}$$

In Eq. (5) and Eq. (6), $C_{1\varepsilon}$, $C_{2\varepsilon}$ and $C_{3\varepsilon}$ are the model constants. Turbulent kinetic energy generations are indicated as G_k and G_b.

$$Re = \frac{\rho v D_h}{\mu} \tag{8}$$

$$Nu = \frac{hD_h}{k} \tag{9}$$

$$f = \frac{\Delta P D_h}{2\rho l v^2} \tag{10}$$

Heat transfer coefficient is calculated from Eq. (11),

$$h = mC_p\left(T_{oavg} - T_{in}\right) / A_s\left(T_{pm} - T_{fm}\right) \tag{11}$$

In Eq. (11), m, MFR for air is

$$m = \rho A_{c/s} V \tag{12}$$

B. Boundary conditions

Solutions to the governing equations {Eqs. (2) to (5)} are numerically obtained. Boundary conditions similar to the actual working conditions are considered for the numerical analysis and given in Table III.

Table III Conditions applied to the boundary

Section	Boundary condition type
Inlet	Velocity inlet
Exit	Pressure outlet
Wall	Adiabatic wall
Absorber Plate	Constant heat flux

SAH exposed to boundary conditions is portrayed in the Fig. 3.

C. Geometric modelling and mesh generation

Geometric modelling is prepared in design modeler in ANSYS FLUENT. Mesh is generated by using mesh tool in FLUENT. The accuracy of the

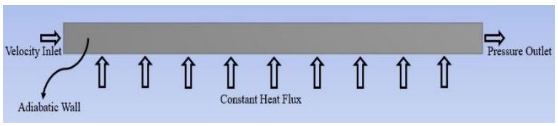

Fig. 3 Boundary conditions

Quantity of cells in the network controls the numerical solution and hence grid independence test is conducted to optimize grid size. Number grids in all three principle directions are varied to get solution to the mesh convergence at a fixed Reynolds number equal to 5000. The results for percentage variation in Nu and f at different total number of grid elements are shown in Table IV. It is found that percentage variation in Nu and f is decreasing with increase in total number of grid elements and it is becoming close to zero as the number of elements are in between 2283840 and 2408832. The optimum grid size is thus selected as 400 along x-axis, 250 along y-axis and 25 along z-axis.

D. Solution methods

Pressure velocity linked CFD solution techniques are used to solve the present problem. Standard k-ε turbulent model with SIMPLE algorithm is used for simultaneous solution of governing equations. Convection terms are controlled by spatial discretization method. Pressure and convection-diffusion terms in the governing equations are discretized using second order central difference. Higher order relaxation is adapted to reduce the computational time.

Present numerical results validated with reproduced corresponding results by Sukhmeet Singh et al. [15] for flow in a rectangular shaped duct with in Fig. 4. It shows good agreement.

Table IV Results of the grid convergence study

Number of elements	*Nu*	Percentage fluctuation of *Nu*	*f*	Percentage fluctuation of *f*
1595370	35.845	1.22	0.0205	2.89
1753752	36.290	0.93	0.0207	2.81
1930275	36.632	1.05	0.0212	2.73
2283840	37.021	0.083	0.0218	0.45
2408832	37.052	0.005	0.0219	0.45
2884440	37.054	0.005	0.0221	0.94
3020160	37.056	--	0.0221	--

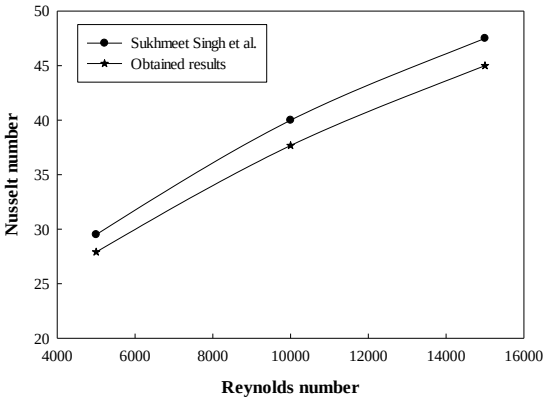

Fig. 4 Assessment of results for validation

4. RESULTS AND DISCUSSION

Heat transmission rates for a conventional Solar airborne heater (SAH) over its absorber plate attached with dissimilar cross sectional ribs which includes rectangle, triangle, semicircular and arc are numerically found. Relative roughness altitude (e/D_h), relative pitch (p/e) and Reynolds' number (Re) in a range of 2300 to 20000 are considered as parametric variables. Boundary conditions given in Table III are applied for all the flow analyses. Results for flow over ribbed absorber plate (with p/e = 10 and e/D_h = 0.055) are compared with corresponding results obtained for flow over plane absorber plate. Optimum rib profile is selected considering enhancement in Nusselt number and decrement in friction factor as the selection parameter. After selecting optimum rib profile, geometrical dimensions of the rib are selected first by varying e/D_h and p/e. Two different e/D_h values equal to 0.073, 0.11 and two different p/e values equal to 6.67, 13.33 are considered to fix the dimensions of the optimized rib profile.

A. Effect of different cross-section of the ribs at constant e/D_h = 0.055 and p/e = 10

Average Nusselt number (Nu) and average friction factor (f) values are numerically found for flow over ribbed absorber plate. Fluctuation of Nu with Re is portrayed in Fig. 5 (a). Similarly fluctuation of f with Re is portrayed in Fig. 5 (b). It also depicts fluctuation of Nu with Re for flow over smooth absorber plate.

Absorber plate provided with arc, semi-circular, rectangular and triangular ribs shows enhancement in Nusselt number (Nu) by 1.66, 1.44, 1.28 and 1.31 times respectively over smooth absorber plate. Similarly it is established from Fig. 5 (b) that, friction factor (f) for absorber plate provided with arc, semi-

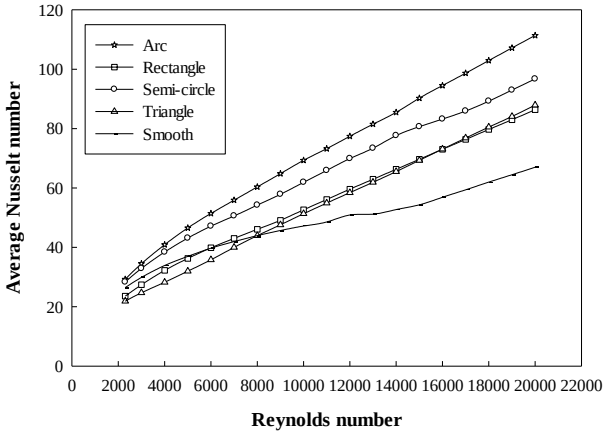

(a) *Re* vs *Nu*

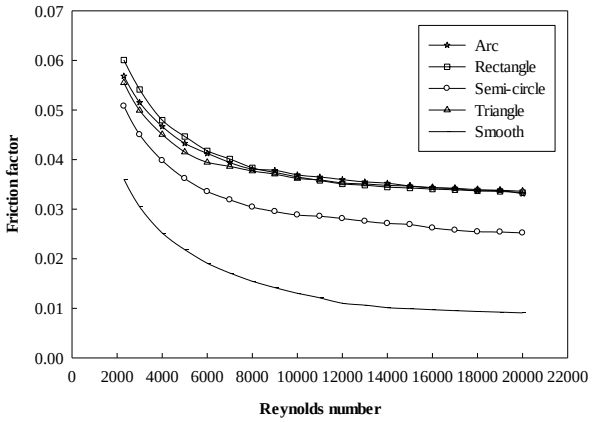

(b) *Re* vs *f*

Fig. 5 Results of SAH with variable profiles of ribs

circular, rectangular and triangular ribs is increased by 3.63, 2.77, 3.67 and 3.70 times respectively over smooth absorber plate. Enhancement in heat transfer rates for flow over absorber plate with arc ribs is found to be higher at e/D_h = 0.055 and p/e = 10. Whereas, enhancement in heat transfer rates is minimum for absorber plate with semi-circular ribs for same values of e/D_h and p/e.

Ribs on the absorber plate will enhance turbulence near the plate and hence reduces high viscous flow layers near the plate. It is concluded from the primary investigations that ribs provided on absorber plate will enhance the heat transfer rate. Absorber plate with arc ribs are considered to the best among all other different rib profiles as it is giving maximum enhancement in Nu and minimum enhancement in f at all different combinations of e/D_h and p/e. In the next stage of analysis physical dimensional of the arc ribs in terms of their relative roughness pitch and relative roughness altitude are optimized.

B. Effect of e/Dh for constant value of p/e = 10

Numerical analysis is continued to select optimum physical dimensions for arc ribs by considering boundary conditions given in Table III. *Re* in between 2300 to 20000, e/D_h values equal to 0.055, 0.073, 0.11 and p/e = 10 are considered at his stage of analysis. Average Nusselt number (*Nu*) and average friction factor (*f*) values are numerically found for flow over ribbed absorber plate. Fluctuation of *Nu* with *Re* for different e/D_h is portrayed in Fig. 6 (a). Similarly fluctuation of *f* with *Re* is portrayed in Fig. 6 (b). Fig. 6 (a) and (b) also depicts fluctuation of *Nu* with *Re* for flow over smooth absorber plate. It is found from Fig. 6 that both *Nu* and *f* values are increased with the use of ribs on the absorber plate. Arc ribbed absorber plate with e/D_h equal to 0.055, 0.0733 and 0.11 shows enhancement in *Nu* by 1.66, 1.78 and 1.47 times respectively higher than the smooth absorber plate.

Percentage increase in *Nu* for e/D_h = 0.0733 is 7.34 when compared to SAH with e/D_h of 0.055. Percentage reduction in *Nu* for e/D_h of 0.11 is 11.08 when compared with SAH having e/D_h of 0.055. Percentage reduction in *Nu* for e/D_h of 0.11 is 17.17 when compared with SAH having e/D_h of 0.0733. Hence it is concluded that there is limit on e/D_h value for maximum heat transfer rate. Up to the value of e/D_h equal to 0.0733, *Nu* is found to be augmented and there after the rate of augmentation is being reduced as we go for a value of 0.11. Arc ribbed absorber plate with e/D_h = 0.073 gives maximum enhancement in heat transfer compared to ribbed plate with e/D_h = 0.055 and 0.11.

Arc ribbed absorber plate with e/D_h equal to 0.055, 0.0733 and 0.11 shows enhancement in *f* by 3.63, 4.76 and 7.25 times respectively higher than the smooth absorber plate. It is observed that with increase in e/D_h value *f* is increased. As e/D_h increased from 0.055 to 0.073 and 0.11, '*f*' is increased by 30.93% and 99.46% respectively.

Percentage increment in *Nu* is more compared to percentage decrement in *f* as e/D_h increased from 0.055 to 0.073. Higher energy inputs are required to supply air through SAH at higher *f* values. Hence it is concluded from this stage of numerical analysis that arc ribbed absorber plate with e/D_h = 0.055 gives better enhancement in heat transfer compared to other values of e/D_h.

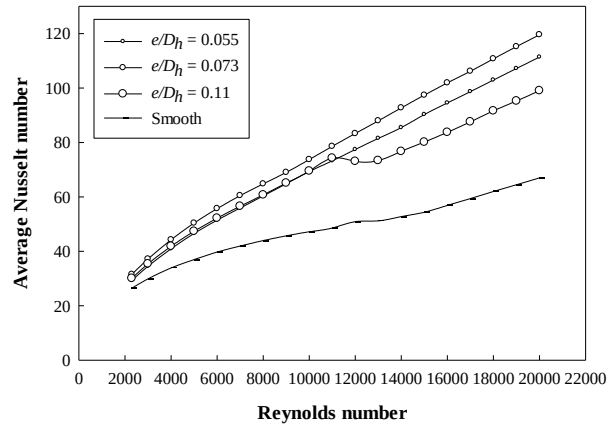

(a) *Re* vs *Nu*

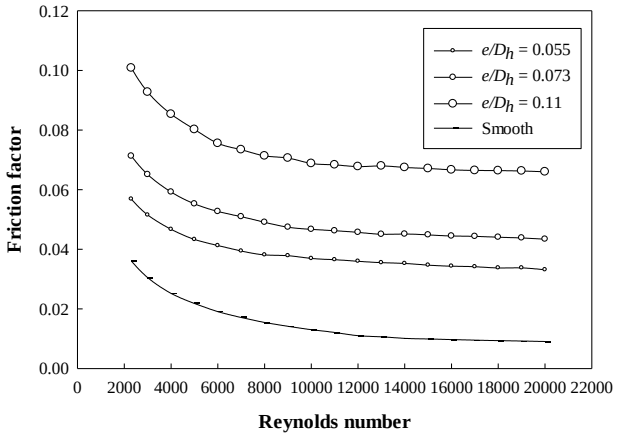

(b) *Re* vs *f*

Fig. 6 Results of SAH with arc ribs on the absorber plate at *p/e* of 10 and e/D_h of 0.055, 0.073 and 0.11

C. Effect of p/e for constant value of e/ Dh = 0.055

Effect of relative roughness tone (p/e) at constant relative roughness altitude (e/D_h) isfound for different values of p/e equal to 6.66, 10 and 13.33. Fluctuation of *Nu* and *f* with *Re* at constant e/D_h and for three different p/e is portrayed in Fig. 7. Extreme enhancement in *Nu* and '*f*' is calculated at each of the assumed p/e value for the analysis of SAH. *Nu* is found to be reduced for $p/e < 10$ and it is found to be increased $p/e > 10$. Maximum enhancement in *Nu* for SAH with arc ribs at constant e/D_h of 0.055 is found to be 1.63, 1.66 and 1.617 at p/e values of 6.67, 10 and 13.33 respectively. It is observed from the results that almost same enhancement is found for p/e. But with p/e value equal to 10 it is observed that SAH is giving better performance when compared with the other two p/e values. Lower values of '*f*' are evaluated to at p/e value of 6.67 and '*f*' is exposed to increase with increase in p/e. Friction factor is found to be increased by 3.43, 3.63 and 3.58 times at p/e of 6.67, 10 and 13.33 respectively. It can be observed that there is only a marginal variation in the *Nu* and '*f*' when changing the p/e values. In the present study the main concentration is on the heat transfer

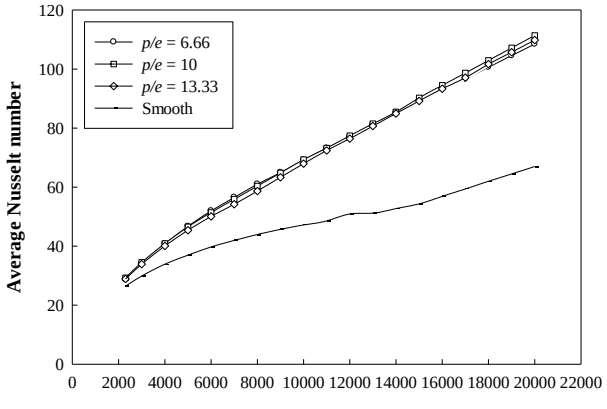

(a) *Re* vs *Nu*

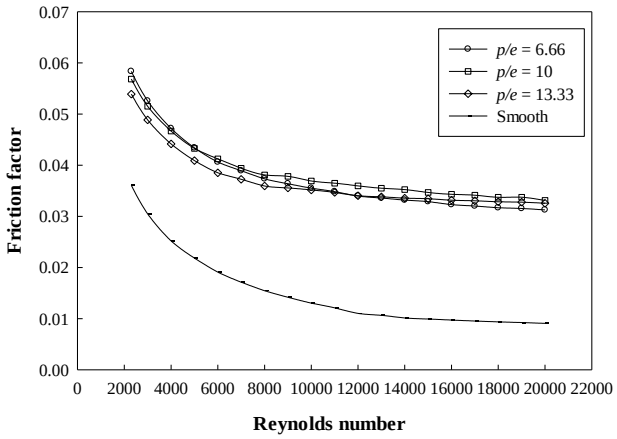

(b) *Re* vs *f*

Fig. 7 Results of SAH with arc ribs on the absorber plate at e/D_h = 0.055 and *p/e* = 6.67, 10 and 13.33

augmentation of SAH between air and the plate, so preference is given for the *p/e* value at which more heat transfer is observed. Thus, it is stated that arc ribs at *p/e* of 10 are giving best performance.

5. CONCLUSION

Forced convection flow through Solar airborne heater is simulated through a rectangular shaped duct with its bottom most surface exposed to constant heat fluctuation boundary. Numerical results are analyzed to know the change in heat transfer for flow though rectangular shaped duct with and without the dissimilar shaped ribs on its bottom most surface. Ribs of different geometries including rectangular, semi-circular, triangular and arc are considered for the numerical analysis. Relative roughness altitude and pitch along with Reynolds number are considered as input parametric variables. Augmentation of Nusselt's number and friction factor variation is considered as output parameters for selecting optimum rib profile and fixing the dimensions of the ribs.

At a fixed roughness pitch value equal to 10 arc ribbed absorber plate is having better heat transfer rates at relative roughness altitude equal to 0.055 when compared to 0.073 and 0.11. Average value of Nusselt's number and average value of friction factor are increased by 1.66, 3.63 times respectively. It has also been found that heat transference enhancement is independent of relative roughness pitch at all Reynolds number. Nusselt's number and friction factor upsurges with upsurge in Reynolds' number for all selected rib profiles.

REFERENCES

1. Varun, R.P. Saini, S.K. Singal, "Investigation of thermal performance of solar airborne heater and transverse ribs on the absorber plate", Renewable Energy, Vol. 33, pp. 1398–1405, 2008.
2. B. N, Prasad and J. S. Saini, "Effect of artificial roughness in a solar airborne heater", Solar Energy, Vol. 41, No. 6. pp. 555-560. 1988.
3. Dhananjay Gupta, S. C. Solanki and J. S. Saini, "Heat and fluid flow in rectangular shape solar airborne heater with transverse rib on absorbant plates", Solar Energy, Vol. 51, No. 1, pp. 31-37, 1993.
4. Atul Lanjewar, J.L. Bhagoria and R.M. Sarviya, "Heat transfer and friction in solar airborne heater duct on absorber plate" Energy, Vol. 36, pp. 4531-4541, 2011.
5. Abdul-Malik Ebrahim Momin, J.S. Saini, S.C. Solanki, "Heat transfer and friction in solar airborne heater duct with V-shaped rib roughness on absorber plate", International Journal of Heat and Mass Transfer, Vol. 45, pp. 3383–3396, 2002.
6. B.K. Gandhi, K.R. Aharwal, and J.S. Saini, "Experimental investigation on heat-transfer enhancement due to a gap in a rectangular shaped duct of solar airborne heater", Renewable Energy, Vol. 33, pp. 585–596, 2008
7. R.S.Gill, V.S.Hans, J.S.Saini and Sukhmeet Singh, "Investigation on performance enhancement in a broken arc rib roughened solar airborne heater duct" Renewable Energy, Vol. 104, pp. 148-162, 2017.
8. Khushmeet Kumar, D.R. Prajapati and Sushant Samir, "Heat transfer and friction factor correlations for solar airborne heater duct with 'S' shaped ribs" Thermal and Fluid Science.
9. Inderjeet Singh, Sukhmeet Singh, "CFD analysis of solar airborne heater duct with transverse ribs as roughness elements", Solar Energy, Vol. 162, pp. 442–453, 2018.
10. Anil Singh Yadav and J.L. Bhagoria, "Heat transfer and fluid flow analysis of solar airborne heater", Renewable and Sustainable Energy Reviews, Vol. 23, pp. 60–79, 2013.
11. Sharad Kumar and R.P. Saini, "CFD based performance analysis of a solar airborne heater duct with artificially synthesized roughness", Renewable Energy, Vol. 34, pp. 1285–1291, 2009.
12. Tabish Alam and Man-Hoe Kim, "Heat transfer enhancement in solar airborne heater duct ", Applied Thermal Engineering, Vol. 126, pp. 458–469, 2017.
13. Tabish Alam and Man-Hoe Kim, "Numerical study on thermal hydraulic performance improvement in solar airborne heater duct ", Energy, Vol. 112, pp. 588-598, 2016.
14. Dongxu Jin, Manman Zhang, Ping Wang and Shasha Xu, "Numerical investigation of heat transfer and fluid flow in a solar airborne heater duct " Energy xxx, pp.1-13, 2015.
15. Sukhmeet Singh, Bikramjit Singh, V.S. Hans and R.S. Gill, "CFD (computational fluid dynamics) investigation on Nusselt number and friction factor of solar airborne heater duct ", Energy xxx, pp.1-9, 2015.
16. K.R. Aharwal, Bhupendra K. Gandhi and J.S. Saini, "Heat transfer and friction characteristics of solar airborne heater ducts ribs on absorber plate", International Journal of Heat and Mass Transfer, Vol. 52, pp. 5970–5977, 2009.
17. Anil Singh Yadav and J.L. Bhagoria, "A CFD based analysis of an artificially roughened solar airborne heater having equilateral triangular sectioned rib", International Journal of Heat and Mass Transfer, Vol. 70, pp.1016–1039, 2014.
18. V.S. Hans, R.S. Gill and Sukhmeet Singh, "Heat transfer and friction factor correlations for a solar airborne heater duct", Experimental Thermal and Fluid Science, Vol. 80, pp. 77–89, 2017.
19. Alok Chaube, P.K. Sahoo, and S.C. Solanki, "Analysis of heat transfer augmentation and flow characteristics due to rib roughness", Renewable Energy, Vol.31, pp. 317–331, 2006.
20. A.Banzaoui and A.Boulemates-Boukadoum , "CFD based analysis of heat transfer enhancement in a solar heater", Energy procedia, Vol.50, pp.761 – 772, 2014.
21. Sompol Skullong, Chinaruk Thianpong and Pongjet Promvonge, "Effects of rib size and its arrangement on in a solar airborne heater channel", Heat Mass Transfer, DOI 10.1007/s00231-015-1515-5.
22. Vipin B. Gawande, A.S. Dhoble, D.B. Zodpe and Sunil Chamoli, "Experimental and CFD investigation of convection heat transfer" Solar Energy, Vol. 131, pp. 275–295, 2016.
23. Mohan Jagadeesh Kumar Mandapati, Lakshmi Pathi Jakkamputi, "Improving the performance of jaggery making unit using solar energy", Perspectives in science, Vol. 8, pp. 146-150, 2016.
24. J.L. Bhagoria, J.S. Saini and S.C. Solanki, "Heat transfer coefficient and friction factor correlations for rectangular solar airborne heater duct", Renewable Energy, Vol. 25, pp.341–369, 2002.
25. Brij Bhushan and Ranjit Singh, "Nusselt number and friction factor correlations for solar airborne heater duct", Solar Energy, Vol.85, pp. 1109–1118, 2011.

Published By:
Blue Eyes Intelligence Engineering
& Sciences Publication